

Contrastive CFG: Improving CFG in Diffusion Models by Contrasting Positive and Negative Concepts

Jinho Chang
KAIST
Seoul, South Korea
jinhojsk515@kaist.ac.kr

Hyungjin Chung
KAIST
Seoul, South Korea
hj.chung@kaist.ac.kr

Jong Chul Ye
KAIST
Seoul, South Korea
jong.ye@kaist.ac.kr



Figure 1. Image samples generated from StableDiffusion 1.5 using *positive prompts* (written in black) and *negative prompts* (written in red), across various negative sampling methods. While some images generated by negated CFG are satisfactory, both DNG and negated CFG show limitations: DNG often fails to negate unwanted concepts effectively, and negated CFG frequently causes severe image quality degradation. In contrast, our proposed guidance term successfully removes undesirable features while preserving the quality of the output image.

Abstract

As Classifier-Free Guidance (CFG) has proven effective in conditional diffusion model sampling for improved condition alignment, many applications use a negated CFG term to filter out unwanted features from samples. However, simply negating CFG guidance creates an inverted probability distribution, often distorting samples away from the marginal distribution. Inspired by recent advances in conditional diffusion models for inverse problems, here we present a novel method to enhance negative CFG guidance using contrastive loss. Specifically, our guidance term aligns or repels the denoising direction based on the given condition through contrastive loss, achieving a nearly identical guiding direction to traditional CFG for positive guidance while overcoming the limitations of existing nega-

tive guidance methods. Experimental results demonstrate that our approach effectively removes undesirable concepts while maintaining sample quality across diverse scenarios, from simple class conditions to complex and overlapping text prompts.

1. Introduction

Classifier-Free Guidance (CFG) [18] forms the key basis of modern text-guided generation with diffusion models. From Bayes rule, CFG constructs a Bayesian classifier $\nabla_{\mathbf{x}} \log p(\mathbf{c}|\mathbf{x}) = \nabla_{\mathbf{x}} \log p(\mathbf{x}|\mathbf{c}) - \nabla_{\mathbf{x}} \log p(\mathbf{x})$ without training additional external classifiers [10]. In practice, it is common to emphasize the classifier vector direction with some constant γ , which corresponds to sharpening the posterior, i.e. $p(\mathbf{x})p(\mathbf{c}|\mathbf{x})^\gamma$. While this may potentially distort

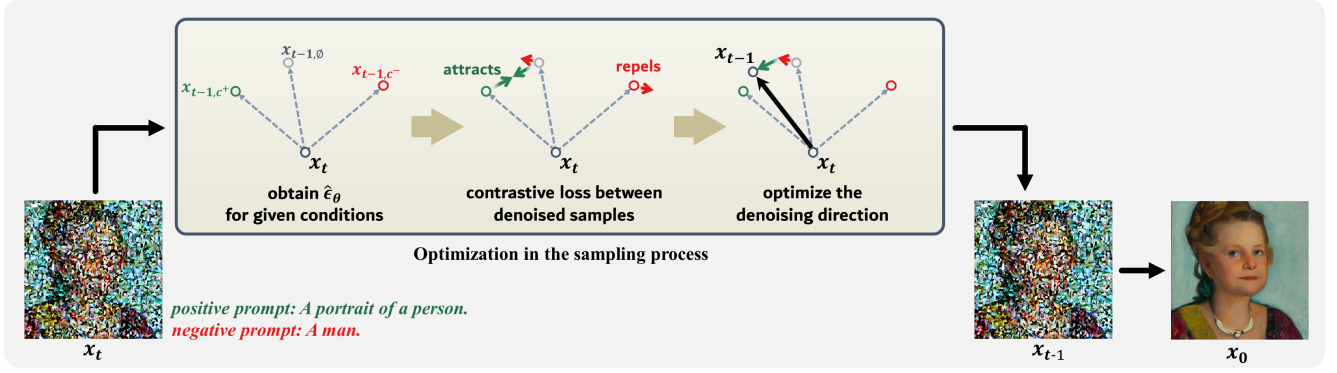


Figure 2. **Overview of the proposed guided sampling of CCFG.** We pose guided sampling as an optimization problem that minimizes the contrastive loss of the positive and negative prompts, which has no computational overhead, yet avoids pitfalls of previous strategies such as negative CFG.

the sampling distribution [11], it is known that the sample quality along with the text alignment increases.

While CFG was originally devised for *adhering* to the target condition, more often than not, there are cases where it is desirable to *avoid* sampling from some conditions. Canonical examples include conditions that describe the poor quality of the image [42], or conditions that are related to harmful content [13, 43]. Often referred to as “negative prompts”, most implementations simply negate the vector direction of CFG, corresponding to inversely weighting with the classifier probability, i.e. $p(\mathbf{x})/p(\mathbf{c}|\mathbf{x})^\gamma$.

Nonetheless, such naïve implementation often leads to a decrease in the sample quality [1, 22]. In this paper, we argue that there are indeed substantial flaws when we choose high values of γ . Specifically, from a distribution standpoint, sampling from $p(\mathbf{x})/p(\mathbf{c}|\mathbf{x})^\gamma$ leads to sampling from the low-density region. Even worse, it may lead to sampling from outside the support of the density. Finally, the negative guidance uses an unbounded objective function when viewed from an optimization standpoint [9, 23].

To mitigate these drawbacks, by leveraging the recent advances in diffusion-based inverse problem solvers (DIS) [7, 8, 21, 23, 39], we reformulate the negative guidance as an inverse problem with a negative prompt-conditioned contrastive loss [5, 15] and derive a reverse diffusion sampling strategy by utilizing decomposed diffusion sampling (DDS) [8]. This results in a simple modification of CFG to the sampling process with little computational overhead. The resulting process, termed *Contrastive CFG (CCFG)*, optimizes the denoising direction by attracting or repelling the denoising direction for the given condition. Furthermore, the attracting and repelling forces are automatically controlled along the sampling process. Through extensive experiments, we verify that CCFG can successfully avoid undesirable concepts while preserving the sample quality.

2. Related works

2.1. Diffusion models

Diffusion models [19, 40] are a class of generative models that learn the score function [20] of the data distribution, and use this score function to revert the forward noising process. The forward process, denoted with the time index t , is governed by a Gaussian kernel that the underlying data distribution $p(\mathbf{x}_0) \equiv p(\mathbf{x})$ eventually approximates the standard normal distribution at time $t = T$, i.e. $p(\mathbf{x}_T) \approx \mathcal{N}(0, \mathbf{I})$. The variance preserving forward transition kernel [19] is given as $p(\mathbf{x}_t|\mathbf{x}_0) = \mathcal{N}(\mathbf{x}_t; \sqrt{\bar{\alpha}_t}\mathbf{x}_0, (1 - \bar{\alpha}_t)\mathbf{I})$. The reverse generative process follows a stochastic differential equation (SDE) [40] governed by the score function $\nabla_{\mathbf{x}_t} \log p(\mathbf{x}_t)$. To estimate this score function, one typically uses epsilon matching [19]

$$\theta^* = \arg \min_{\theta} \mathbb{E} [\|\epsilon_{\theta}(\sqrt{\bar{\alpha}_t}\mathbf{x}_0 + \sqrt{1 - \bar{\alpha}_t}\epsilon) - \epsilon\|_2^2], \quad (1)$$

which can be shown to be equivalent to denoising score matching [41], $s_{\theta}(\mathbf{x}_t) = \nabla_{\mathbf{x}_t} \log p(\mathbf{x}_t) = -\frac{1}{\sqrt{1 - \bar{\alpha}_t}}\epsilon_{\theta}(\mathbf{x}_t)$. By Tweedie’s formula [12], one can recover the posterior mean $\hat{\mathbf{x}}(\mathbf{x}_t) = \mathbb{E}[\mathbf{x}_0|\mathbf{x}_t] = \frac{1}{\sqrt{\bar{\alpha}_t}}(\mathbf{x}_t - \sqrt{1 - \bar{\alpha}_t}\epsilon_{\theta}(\mathbf{x}_t))$. Moreover, it is common practice to train a *conditional* score function conditioned on the text prompt [18] with random dropping to use it flexibly, either as $\epsilon_{\theta}(\mathbf{x}_t, \mathbf{c})$ or $\epsilon_{\theta}(\mathbf{x}_t) := \epsilon_{\theta}(\mathbf{x}_t, \emptyset)$, where \emptyset refers to the null condition. In practice, a popular way of generating images through reverse sampling is through DDIM sampling [38], where a single iteration can be written as

$$\hat{\mathbf{x}}_{\emptyset}(\mathbf{x}_t) = (\mathbf{x}_t - \sqrt{1 - \bar{\alpha}_t}\epsilon_{\theta}(\mathbf{x}_t, \emptyset))/\sqrt{\bar{\alpha}_t} \quad (2)$$

$$\mathbf{x}_{t-1} = \sqrt{\bar{\alpha}_{t-1}}\hat{\mathbf{x}}_{\emptyset}(\mathbf{x}_t) + \sqrt{1 - \bar{\alpha}_{t-1}}\epsilon_{\theta}(\mathbf{x}_t, \emptyset), \quad (3)$$

where we defined $\hat{\mathbf{x}}_{\emptyset}(\mathbf{x}_t)$ as the posterior mean without the conditioning. Iterating (2) and (3) amounts to sampling from $p(\mathbf{x})$.

2.2. Classifier-free guidance

Plugging in the conditional epsilon $\epsilon_\theta(\mathbf{x}_t, \mathbf{c})$ to sample from the conditional distribution $p(\mathbf{x}|\mathbf{c})$ does not work well in practice, due to the guidance effect being too weak. To mitigate this downside, it is standard to use classifier-free guidance (CFG) [18] at sampling time. The key idea is to use

$$\hat{\epsilon}_{c^+}^\gamma(\mathbf{x}_t) := \hat{\epsilon}_\emptyset(\mathbf{x}_t) + \gamma(\hat{\epsilon}_{c^+}(\mathbf{x}_t) - \hat{\epsilon}_\emptyset(\mathbf{x}_t)), \quad (4)$$

where we defined $\hat{\epsilon}_c(\mathbf{x}_t) := \epsilon_\theta(\mathbf{x}_t, \mathbf{c})$ ¹. Running DDIM sampling with $\hat{\epsilon}_{c^+}^\gamma(\mathbf{x}_t)$ in the place of $\hat{\epsilon}_\emptyset(\mathbf{x}_t)$ leads to sampling from the gamma-powered distribution $p^\gamma(\mathbf{x}|c^+) := p(\mathbf{x})p(c^+|\mathbf{x})^\gamma$, a sharpened posterior. This way, adherence to the condition c^+ is emphasized.

2.3. Guided sampling

Another popular way of posterior sampling with diffusion models is to use guided sampling, where the guidance is given by the gradient of some energy function [7, 36, 46, 48]. Denoting $\ell(\cdot)$ as the energy to be minimized, guided sampling using Decomposed Diffusion Sampling [8] has the form

$$\mathbf{x}_{t-1} = \sqrt{\bar{\alpha}_{t-1}}(\hat{\mathbf{x}}_\emptyset - \omega_t \nabla_{\hat{\mathbf{x}}_\emptyset} \ell(\hat{\mathbf{x}}_\emptyset)) + \sqrt{1 - \bar{\alpha}_{t-1}} \hat{\epsilon}_\emptyset,$$

where ω_t is the step size. For instance, by using the score distillation sampling (SDS) loss [30], we have

$$\begin{aligned} \ell_{SDS}(\mathbf{x}) &:= \|\epsilon_\theta(\sqrt{\bar{\alpha}_t} \mathbf{x} + \sqrt{1 - \bar{\alpha}_t} \epsilon) - \epsilon\|_2^2 \\ &= \frac{\bar{\alpha}_t}{1 - \bar{\alpha}_t} \|\hat{\mathbf{x}}_c - \mathbf{x}\|_2^2 \end{aligned} \quad (5)$$

leading to the improved version of CFG called CFG++ [9]:

$$\mathbf{x}_{t-1} = \sqrt{\bar{\alpha}_{t-1}}(\hat{\mathbf{x}}_\emptyset + \gamma(\hat{\mathbf{x}}_c - \hat{\mathbf{x}}_\emptyset)) + \sqrt{1 - \bar{\alpha}_{t-1}} \hat{\epsilon}_\emptyset, \quad (6)$$

with $\gamma := \frac{2\bar{\alpha}_t}{1 - \bar{\alpha}_t} \omega_t$, where the only difference from the original CFG is the use of $\hat{\epsilon}_\emptyset$ instead of $\hat{\epsilon}_{c^+}^\gamma$ in (6). In fact, the authors in [9] also showed that the CFG++ is a scaled version of CFG where the improvement is especially dominating at the early stage of reverse sampling. In this regard, CFG sampling with reverse sampling can also be seen as guided sampling with the SDS loss function.

2.4. Concept Negation

Negative guidance. Analogous to emphasize sampling from c^+ in CFG, *negative* guidance aims to avoid sampling from the condition c^- . The simplest case [1, 13, 24, 29] negates the guidance direction in (4) such as

$$\hat{\epsilon}_{c^-}^\gamma(\mathbf{x}_t) := \hat{\epsilon}_\emptyset(\mathbf{x}_t) - \gamma(\hat{\epsilon}_{c^-}(\mathbf{x}_t) - \hat{\epsilon}_\emptyset(\mathbf{x}_t)), \quad (7)$$

¹With a slice abuse of notation, we omit the dependence on \mathbf{x}_t when it is clear from context.

where the goal is to avoid sampling from c^- . Note that this corresponds to sampling from $p^{-\gamma}(\mathbf{x}|c^-) := p(\mathbf{x})/p(c^-|\mathbf{x})^\gamma$, a joint distribution inversely proportional to the posterior likelihood. When the goal is to sample from c^+ while avoiding c^- , one uses [2, 42]

$$\begin{aligned} \hat{\epsilon}_{c^+, c^-}^\gamma &:= \hat{\epsilon}_{c^+} + \gamma(\hat{\epsilon}_{c^+} - \hat{\epsilon}_{c^-}) \\ &= \hat{\epsilon}_{c^+} + \gamma(\hat{\epsilon}_{c^+} - \hat{\epsilon}_\emptyset) - \gamma(\hat{\epsilon}_{c^-} - \hat{\epsilon}_\emptyset) \end{aligned} \quad (8)$$

In both cases, pushing away from c^- is governed by the *negation* of the vector direction $(\hat{\epsilon}_{c^-} - \hat{\epsilon}_\emptyset)$.

Recently, Koulischer et al. [24] proposed dynamic negative guidance (DNG) and proposed sampling from $p(\mathbf{x})(p(-c^-|\mathbf{x}))^\gamma$. Here, $-c^-$ is defined as a condition such that $p(-c^-|\mathbf{x}) = 1 - p(c^-|\mathbf{x})$, which can also be seen as a union of all possible input conditions except c^- . Applying Bayes rule, one can show that

$$\begin{aligned} \nabla_{\mathbf{x}_t} \log p(\mathbf{x}_t | -c^-) &= \nabla_{\mathbf{x}_t} \log p(\mathbf{x}_t) \\ &\quad - \gamma(\mathbf{x}_t, c^-)(\nabla_{\mathbf{x}_t} \log p(\mathbf{x}_t | c^-) - \nabla_{\mathbf{x}_t} \log p(\mathbf{x}_t)), \end{aligned} \quad (9)$$

where

$$\gamma(\mathbf{x}_t, c^-) = \frac{p(c^-|\mathbf{x}_t)}{1 - p(c^-|\mathbf{x}_t)}, \quad (10)$$

which can be approximated during the reverse diffusion process to adjust the guidance scale dynamically.

Negation for safety in Text-to-Image models. Ensuring the safe deployment of text-to-image (T2I) models requires careful avoidance of specific content and concepts [32, 34, 35]. Key risks include potential privacy breaches, copyright violations, and the generation of harmful or inappropriate content [3, 37]. Addressing these concerns necessitates a multi-stage approach spanning pre-training, fine-tuning, and inference. During pre-training, targeted filtering is applied to the dataset to exclude harmful content, though this is both resource-intensive and challenging to enforce exhaustively. At the fine-tuning stage, various *unlearning* techniques have emerged [14, 43, 47], often focusing on modifying specific components, such as the cross-attention layer, to effectively “forget” designated concepts. However, these methods are limited by the difficulty of predefining all undesired concepts. At inference, negative guidance serves as a cost-effective solution to restrict specific content generation without additional model tuning. Our experiments validate the efficacy of our approach within this context, highlighting its practical advantages in managing content safety at deployment.

3. Main Contribution: Contrastive CFG

Limitations of different negative guidance. The downside of the negated CFG (nCFG) term in (7) can be explained in two different aspects: the sampling distribution involves

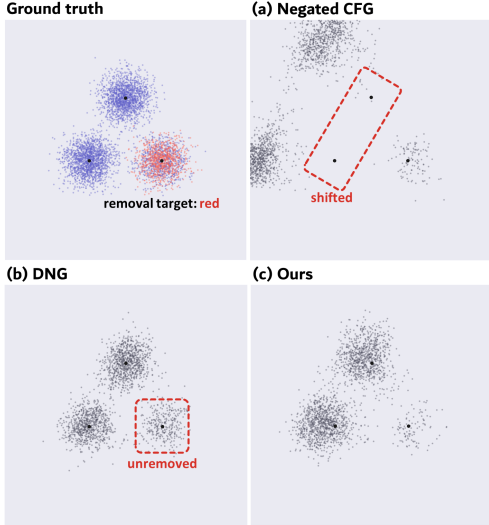


Figure 3. **Output distribution with different negative sampling methods on a manually constructed dataset with two classes.** (a) Negated CFG heavily shifts the samples from the marginal distribution. (b) DNG output still contains samples that can be regarded as the red class. (c) Our method can remove all samples that satisfy a forbidden class while preserving the unrelated distribution.

the inverted probability $p(c^-|\mathbf{x})^{-\gamma}$, which quickly dominates over $p(\mathbf{x})$ as γ grows [24]. This heavily distorts the sampling distribution and possibly moves it off the supports of marginal data distribution. Also, from the perspective of guided sampling [9, 23], the nCFG term can be seen as a guided sampling that minimizes the negative SDS loss, which has no lower bound. This yields a strong repulsive gradient even in regions far from c^- , unnecessarily pushing further away. Figure 3(a) visualizes this issue with a toy dataset consisting of two classes, where two nodes contain the blue class and the other node is mixed with blues and reds. When nCFG sampling was done with the red class, the output distribution avoided the blue node but the other two nodes were entirely shifted from the original location. The ideal behavior of negative guidance is that the strength of the guidance term decreases to zero as \mathbf{x}_t becomes irrelevant to the given condition, being equivalent to unconditional sampling.

Meanwhile, DNG [24] resolved this issue by weighting the nCFG guidance term with (10), which goes to 0 as $p(c^-|\mathbf{x}_t)$ decreases. However, the biggest limitation of DNG is that its sample faithfully avoids c^- only when $p(c^-|\mathbf{x}_t) \approx 1$ for all \mathbf{x}_t that satisfies c^- . If the conditions are not mutually exclusive, the output distribution still includes the data that agrees with c^- . In Figure 3(b), the output distribution still retains the third node with roughly half of the original, because the blue class also exists in the third node. This limitation is especially crucial for text-to-image

Method	Target	Objective	Stability	Precision
nCFG [42]	$\frac{p(\mathbf{x})}{p(c \mathbf{x})}$	$-\ell_{SDS}$		✓
DNG [24]	$p(\mathbf{x} c^-)$	-	✓	
Ours	-	NCE	✓	✓

Table 1. Summary of different training-free negative sampling methods. Stability refers to the sampling distribution not deviating from the marginal support. Precision means the method can thoroughly rule out the sample that has the unwanted feature.

(T2I) models (*e.g.* StableDiffusion [33]) which take a wide range of overlapping prompts, and therefore each prompt has low $p(c|\mathbf{x})$. Sampling from $p(\mathbf{x}|c^-)$ with T2I models cannot rule out the sample with c^- , when the model samples from a very similar but different condition to c^- instead. Also, DNG requires the numerically unstable computation of $p(c^-|\mathbf{x}_t)$ and the condition prior $p(c^-)$, which leads to additional affine hyperparameters and a prior value setting with a lack of justification.

Table 1 summarizes the aforementioned negative guidance. Inverted probability distribution-based methods show high precision on the output for negating the undesired concept, but the guidance retains strongly in the unrelated region and corrupts the marginal distribution. DNG enables a more stable sampling by canceling the guidance scale for irrelevant samples, yet the sample can still be related to the negative prompt as the condition begins to overlap. We aimed to combine the strength of both approaches and present a method that faithfully removes unwanted concepts without changing the sampling odds of unrelated data.

Derivation of CCFG. Similar to redefining positive CFG as a guided sampling that assimilates the denoising direction with the conditioned noise [9, 23], we implement sampling that negates certain conditions with an appropriate objective function. Considering this task as optimizing the data in the sampling process closer or further away from a given condition, we propose to use a contrastive loss [4, 16] as the objective function for positive/negative prompt guidance. Contrastive loss assimilates features with the same context and distances semantically unrelated features, and we found that Noise Contrastive Estimation (NCE) [15] suits the most our situation among various contrastive loss concepts.

Specifically, NCE parameterizes the data by performing logistic regression to discriminate the observed data from the noise data distribution. With a modeled data distribution $p_\theta(\mathbf{x})$ parameterized by θ and pre-defined noise data distribution $q(\mathbf{x})$, the logit of \mathbf{x} for the logistic regression is defined as

$$l(\mathbf{x}) := \log p_\theta(\mathbf{x}) - \log q(\mathbf{x}), \quad (11)$$

which formulates the NCE loss as

$$\begin{aligned}\mathcal{L}_{NCE} &:= -y \log \sigma(l_\theta(x)) - (1-y) \log(1 - \sigma(l_\theta(x))) \\ &= -y \log \frac{p_\theta(\mathbf{x})}{p_\theta(\mathbf{x}) + q(\mathbf{x})} - (1-y) \log \frac{q(\mathbf{x})}{p_\theta(\mathbf{x}) + q(\mathbf{x})}\end{aligned}\quad (12)$$

where y is 1 if \mathbf{x} is the real data and 0 if \mathbf{x} is sampled from $q(\mathbf{x})$. Although NCE mostly updates the model parameter with a given positive or noise data, we optimize a datapoint with a pre-trained model that nicely parameterizes $p_\theta(\mathbf{x})$.

When we denoise the noised data \mathbf{x}_t and guide $\hat{\mathbf{x}}_\emptyset$ to satisfy \mathbf{c} , we set $q(\mathbf{x}) := p(\mathbf{x}_{t-1}|\mathbf{x}_t, \emptyset)$ and parameterize $p_\theta(\mathbf{x})$ with pre-trained diffusion model $p(\mathbf{x}_{t-1}|\mathbf{x}_t, \mathbf{c})$ to optimize ϵ with the corresponding NCE loss²:

$$\ell^+(\epsilon) := -\log \frac{p_\theta(\hat{\mathbf{x}}_{t-1}(\epsilon))}{p_\theta(\hat{\mathbf{x}}_{t-1}(\epsilon)) + q(\hat{\mathbf{x}}_{t-1}(\epsilon))}\quad (13)$$

Here, $\hat{\mathbf{x}}_{t-1}(\epsilon)$ is a mean prediction of \mathbf{x}_{t-1} from \mathbf{x}_t with ϵ . Assuming a small noise level difference between t and $t-1$, [19] states that this can be obtained as follows:

$$\hat{\mathbf{x}}_{t-1}(\epsilon) = \frac{\sqrt{\alpha_{t-1}}}{\sqrt{\alpha_t}} \left(\mathbf{x}_t - \frac{\alpha_{t-1} - \alpha_t}{\alpha_{t-1}\sqrt{1 - \alpha_t}} \epsilon \right)\quad (14)$$

With the same assumption above, we can also get a closed form of $p(\mathbf{x}_{t-1}|\mathbf{x}_t, \emptyset) = \mathcal{N}(\boldsymbol{\mu}_p, \sigma^2)$ and $p(\mathbf{x}_{t-1}|\mathbf{x}_t, \mathbf{c}) = \mathcal{N}(\boldsymbol{\mu}_q, \sigma^2)$, as a Gaussian distribution with a shared variance σ^2 and

$$\boldsymbol{\mu}_p = \frac{\sqrt{\alpha_{t-1}}}{\sqrt{\alpha_t}} \left(\mathbf{x}_t - \frac{\alpha_{t-1} - \alpha_t}{\alpha_{t-1}\sqrt{1 - \alpha_t}} \hat{\mathbf{c}} \right)\quad (15)$$

$$\boldsymbol{\mu}_q = \frac{\sqrt{\alpha_{t-1}}}{\sqrt{\alpha_t}} \left(\mathbf{x}_t - \frac{\alpha_{t-1} - \alpha_t}{\alpha_{t-1}\sqrt{1 - \alpha_t}} \hat{\mathbf{c}}_\emptyset \right)\quad (16)$$

Therefore, the loss function in (13) can be simplified as

$$-\log \frac{e^{-\|\hat{\mathbf{x}}_{t-1}(\epsilon) - \boldsymbol{\mu}_p\|_2^2 / 2\sigma^2}}{e^{-\|\hat{\mathbf{x}}_{t-1}(\epsilon) - \boldsymbol{\mu}_p\|_2^2 / 2\sigma^2} + e^{-\|\hat{\mathbf{x}}_{t-1}(\epsilon) - \boldsymbol{\mu}_q\|_2^2 / 2\sigma^2}}\quad (17)$$

$$= -\log \frac{e^{-\tau\|\epsilon - \hat{\mathbf{c}}\|_2^2}}{e^{-\tau\|\epsilon - \hat{\mathbf{c}}\|_2^2} + e^{-\tau\|\epsilon - \hat{\mathbf{c}}_\emptyset\|_2^2}}\quad (18)$$

Here, τ is a coefficient that can depend on the noise scheduling and also additional user parameters as the ‘‘temperature’’ on the logit [5]. Although τ can be defined as timestep-dependent based on the diffusion reverse process, we found that setting τ as a constant yields stable and preferable results, while being simple to implement.

²Though many works on guided sampling for inverse problems defined their loss on the posterior mean, the guidance on these losses are linearly related to the guidance on $\hat{\mathbf{c}}_\emptyset$ since posterior mean is a linear combination of \mathbf{x}_t and $\hat{\mathbf{c}}_\emptyset$.

Algorithm 1 DDIM sampling with CCFG

Require: $\mathbf{x}_T \sim \mathcal{N}(0, \mathbf{I}), \omega > 0, \tau > 0, \text{mode} \in \{\text{‘pos’}, \text{‘neg’}\}$

- 1: Initialize $\mathbf{x}_t = \mathbf{x}_T$
- 2: **for** $i = T$ **to** 1 **do**
- 3: **if** mode == ‘pos’ **then**
- 4: $\lambda = \frac{2}{1 + e^{-\tau\|\hat{\mathbf{c}}_\emptyset(\mathbf{x}_t) - \hat{\mathbf{c}}(\mathbf{x}_t)\|_2^2}}$
- 5: **else**
- 6: $\lambda = -\frac{2e^{-\tau\|\hat{\mathbf{c}}_\emptyset(\mathbf{x}_t) - \hat{\mathbf{c}}(\mathbf{x}_t)\|_2^2}}{1 + e^{-\tau\|\hat{\mathbf{c}}_\emptyset(\mathbf{x}_t) - \hat{\mathbf{c}}(\mathbf{x}_t)\|_2^2}}$
- 7: **end if**
- 8: $\hat{\mathbf{c}}_\mathbf{c}^\omega(\mathbf{x}_t) = \hat{\mathbf{c}}_\emptyset(\mathbf{x}_t) + \omega\lambda(\hat{\mathbf{c}}_\mathbf{c}(\mathbf{x}_t) - \hat{\mathbf{c}}_\emptyset(\mathbf{x}_t))$
- 9: $\hat{\mathbf{x}}_\mathbf{c}^\omega(\mathbf{x}_t) = (\mathbf{x}_t - \sqrt{1 - \bar{\alpha}_t}\hat{\mathbf{c}}_\mathbf{c}^\omega(\mathbf{x}_t))/\sqrt{\bar{\alpha}_t}$
- 10: $\mathbf{x}_t = \sqrt{\bar{\alpha}_{t-1}}\hat{\mathbf{x}}_\mathbf{c}^\omega(\mathbf{x}_t) + \sqrt{1 - \bar{\alpha}_{t-1}}\hat{\mathbf{c}}_\mathbf{c}^\omega(\mathbf{x}_t)$
- 11: **end for**
- 12: **return** \mathbf{x}_t

We take the derivative with respect to ϵ computed at $\epsilon = \hat{\mathbf{c}}_\emptyset$ as a positive guidance term, which can be obtained in closed form as follows.

$$\hat{\mathbf{c}}_{\mathbf{c}, \ell^+}^{\gamma, \tau} := \hat{\mathbf{c}}_\emptyset - \omega_t \nabla_\epsilon \ell^+(\hat{\mathbf{c}}_\emptyset)\quad (19)$$

$$= \hat{\mathbf{c}}_\emptyset + \frac{2\gamma}{1 + e^{-\tau\|\hat{\mathbf{c}}_\emptyset - \hat{\mathbf{c}}_\mathbf{c}\|_2^2}} (\hat{\mathbf{c}}_\mathbf{c} - \hat{\mathbf{c}}_\emptyset)\quad (20)$$

Here, $\gamma := \tau\omega_t$ is a set of hyperparameters which works as a whole for guidance scale in conventional CFG.

Similarly, to utilize the same objective function to avoid \mathbf{c} , we set $q(\mathbf{x})$ and $p_\theta(\mathbf{x})$ the same as above but treat \mathbf{x}_t as a sample from $q(\mathbf{x})$. When we perform gradient descent on $\hat{\mathbf{c}}_\emptyset$ to minimize the following loss term, we get

$$\ell^-(\epsilon) := -\log \frac{q(\hat{\mathbf{x}}_{t-1}(\epsilon))}{p_\theta(\hat{\mathbf{x}}_{t-1}(\epsilon)) + q(\hat{\mathbf{x}}_{t-1}(\epsilon))}\quad (21)$$

$$= -\log \frac{e^{-\tau\|\epsilon - \hat{\mathbf{c}}_\emptyset\|_2^2}}{e^{-\tau\|\epsilon - \hat{\mathbf{c}}_\mathbf{c}\|_2^2} + e^{-\tau\|\epsilon - \hat{\mathbf{c}}_\emptyset\|_2^2}}\quad (22)$$

which results in the following update:

$$\hat{\mathbf{c}}_{\mathbf{c}, \ell^-}^{\gamma, \tau} := \hat{\mathbf{c}}_\emptyset - \frac{2\gamma e^{-\tau\|\hat{\mathbf{c}}_\emptyset - \hat{\mathbf{c}}_\mathbf{c}\|_2^2}}{1 + e^{-\tau\|\hat{\mathbf{c}}_\emptyset - \hat{\mathbf{c}}_\mathbf{c}\|_2^2}} (\hat{\mathbf{c}}_\mathbf{c} - \hat{\mathbf{c}}_\emptyset).\quad (23)$$

Algorithm 1 congregates two scenarios and performs reverse sampling to satisfy or remove the given condition \mathbf{c} . Compared to the conventional CFG, an additional weighting coefficient was added to the guidance term of each step. In the region where $\|\hat{\mathbf{c}}_\emptyset(\mathbf{x}_t) - \hat{\mathbf{c}}_\mathbf{c}(\mathbf{x}_t)\|_2^2$ is small, the coefficient is close to 1 in both positive and negative cases. As $\|\hat{\mathbf{c}}_\emptyset(\mathbf{x}_t) - \hat{\mathbf{c}}_\mathbf{c}(\mathbf{x}_t)\|_2^2$ grows significant in the process of negative sampling, the coefficient goes to 0 and becomes unconditional sampling. More analysis on the suggested objective functions can be found in Section 5.



Figure 4. The plot between the error rate and FID for nCFG, DNG, and CCFG on class-removal negative sampling, in MNIST and CIFAR10 datasets. The numbers on the plots refer to the guidance scales. Starting from the lower right, all three sampling methods share the same guidance scales, which are written as the numbers on the plots.

4. Experimental results

In this section, we tested how the suggested guidance term can steer the sample to satisfy or exclude the certain condition, along with its effect into the sample quality. We tested the nCFG and DNG for the baseline comparison, as they are best fit for the scope of training-free diffusion sampling methods for concept negation. Although our derivation is based on (5) and requires the use of CFG++, for a fair comparison with nCFG and DNG which are based on CFG, we conduct experiments using the original CFG across a range of scenarios where CFG is applicable, including class-conditioned image generation and text-to-image (T2I) generation. In the Supplementary material, we also provide a CFG++ version of CCFG to validate its theoretical correctness. All experiments were performed with deterministic DDIM sampling.

Guidance on class-conditioned models. To examine the performance of CCFG on class-conditioned diffusion models, two different image datasets of MNIST [26] and CIFAR10 [25] were considered. Both dataset comprises 10 classes which are relatively exclusive to each other.

We first trained a diffusion model based on DDPM [19] for each dataset, that can perform both conditional and unconditional generation to enable CFG. After the generator is trained, we apply different negative sampling methods to each class and calculate the error rate of 1,000 samples, which is the portion of the samples that match the forbidden class according to separately prepared external classifiers. The mean error rate for all 10 classes is measured for the precision of the utilized negative sampling method. To quantify the output image quality, we measured the Fréchet Inception Distance (FID) [17] between 10,000 sampled images and the real data. The DDPM models were trained with 500 noise timesteps. For sampling, DDIM sampling [38]

	Negative Guidance	pos. prompt[↑] HPS-v2	GPT4	neg. prompt[↓] HPS-v2	GPT4
(a)	None	0.260	1.00	0.213	0.10
	DNG	0.258	0.99	0.211	0.09
	nCFG	0.220	0.66	0.158	0.00
	CCFG	0.251	0.99	0.184	0.00
(b)	None	0.322	0.99	0.232	0.75
	DNG	0.312	1.00	0.219	0.31
	nCFG	0.297	0.85	0.192	0.01
	CCFG	0.314	1.00	0.204	0.02
(c)	None	0.258	0.99	0.192	0.45
	DNG	0.257	0.99	0.189	0.38
	nCFG	0.241	0.90	0.173	0.01
	CCFG	0.246	0.96	0.175	0.04
(d)	None	0.254	1.00	0.271	0.94
	DNG	0.252	1.00	0.266	0.87
	nCFG	0.222	0.89	0.179	0.00
	CCFG	0.235	0.99	0.205	0.03

Table 2. Qualitative evaluation results with 100 sampled images on each scenario in Figure 1.

with NFE=100 was used. For CCFG sampling, we set τ as a constant of 0.2. We re-implemented DNG to work on DDIM sampling and used the hyperparameter configuration with the lowest error rate we’ve tested, which we report in the Supplementary material.

For three negative sampling methods, we plotted the curve of error rate versus FID with varying guidance scales in Figure 4. For all datasets and sampling methods, the increased guidance scale reduced the error rate but damaged the FID. This trade-off between the precision and sample quality is consistent with the observations reported in conventional CFG. The curve of CCFG is located at the bottom left in both MNIST and CIFAR10, outperforming the nCFG and previously suggested DNG. Except for a too-small guidance scale where the error rate was not sufficiently low, CCFG achieved similar or better precision than the other two with higher sample quality.

Guidance on text-to-image models. In this section, we test the performance of CCFG in the context of T2I generation, where the conditioning signal is much more complex and intertwined. In the T2I case, existing conditions are far from being mutually exclusive, and there are many cases where there is some vague overlap between the conditions that we would like to generate and the ones that we would like to refrain from. All experiments were conducted using StableDiffusion (SD)1.5. For sampling, we used DDIM with 50 NFE with a guidance scale of 7.5. For DNG, we used the hyperparameter configuration provided from the authors.

In Figure 1, we illustrate the results of negative sampling obtained by using nCFG, DNG and CCFG in SD1.5. We found that DNG often cannot faithfully remove the concept in the negative prompt. Due to the characteristic of the overlapping text condition, the calculated guidance scale of DNG was insufficient to repel the output from the unwanted

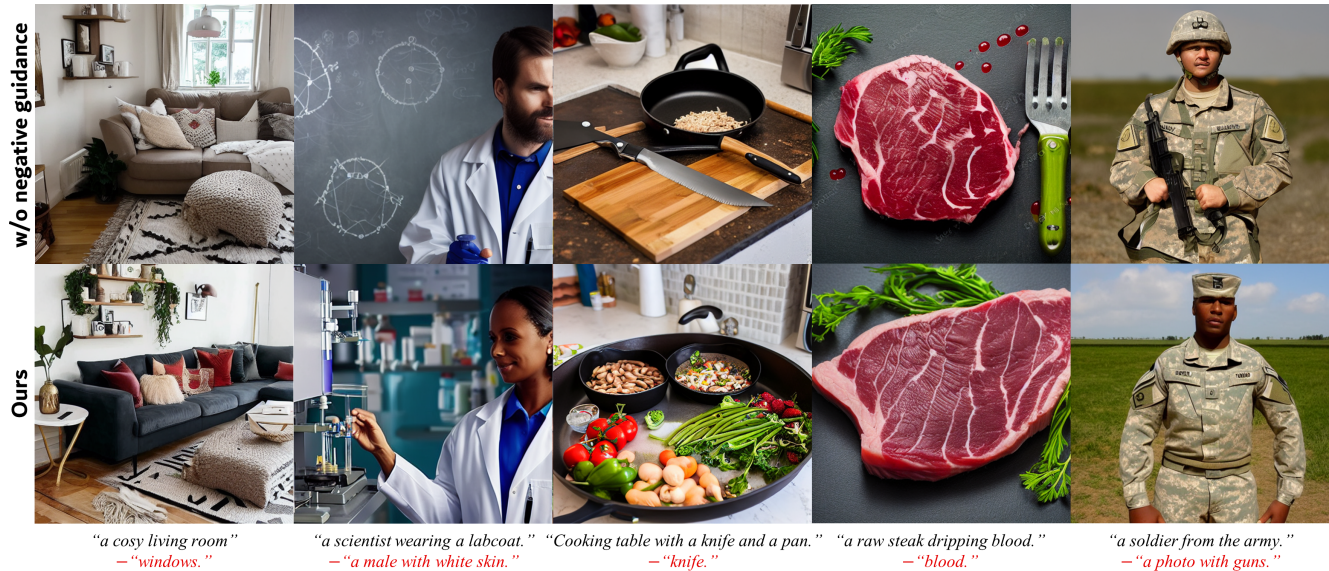


Figure 5. Examples of SD1.5 generation results with positive-negative prompt pairs and CCFG to remove various features such as objects, internal bias, and potentially unsuitable contents.

features. In the case of nCFG, we observe three downsides: in the first scenario of Figure 1, the use of negative prompts hamper the affinity to the positive prompt. In the second scenario, we bias in the samples due to the exaggerated negative guidance direction, resulting in removing *all* red fruits from the image. Finally, we observe the quality of the images is degraded heavily overall.

To evaluate this difference quantitatively, we sample 100 images for each prompt provided in the figure. As the alignment metric between the generated images with the text prompts, we used HPS-v2 [44]. We note that we also tried other similar metrics such as CLIP score [31] or ImageReward [45], and found similar trends. We report the results using all these metrics in the Supplementary material. These metrics behave as a meaningful proxy to evaluate the faithfulness to the positive prompts. However, note that for the alignment score with the negative prompt, we want *lower* scores, indicating that the image does not contain the concept. Nevertheless, it is hard to tell if the low score is attributed to successfully avoiding the generation of certain concepts, or simply due to the low image quality. To mitigate this limitation, as proposed in several recent works, we adopt the VLM-as-a-judge framework [6, 27]. Specifically, we used GPT4 and used as input the prompt and the sampled image, asking the model whether the sampled image contained the attribute. We asked the language model to decompose the given text prompt, and then check the given image’s agreement with each component to eventually rate the image on a scale of 0 to 1. Detailed prompts and the evaluation protocol can be found in the Supplementary material. In Tab. 2, we see that the alignment with the positive

prompt is much higher in CCFG as opposed to the case of nCFG. Moreover, although the HPS-v2 metric in the negative prompt is lower for the case of nCFG, the evaluation with GPT4 shows that the results are actually comparable. Compared to the GPT4 score with no negative guidance, this implies that CCFG is sufficient to remove the undesired properties, and the lower HPS-v2 score for the nCFG can partly be attributed to the degraded image quality.

Figure 5 shows additional image generation scenarios with CCFG from SD1.5. Note that leveraging the ability of CCFG of effective and stable concept negation, we can resolve certain undesired features including a potential bias in the generative model itself or inappropriate contents. Figure 5 demonstrates that CCFG can help the model generate minority samples and remove harmful objects by suitable negative prompts.

For extensive and thorough evaluation beyond case studies, we used 10k COCO [28] prompts to test the alignment against positive and negative prompts. Since only the positive prompts are provided in the COCO dataset, we synthesized positive-negative prompt pairs with GPT4 to test the effect of negative sampling. Specifically, GPT4 first lists all visual objects in the given COCO caption, and then removes a randomly selected object from the original caption to build a positive prompt and negative prompt for the removed object. We provide the details of generating this benchmark in the Supplementary material. Tab. 3 shows the quantitative metrics of nCFG, DNG and CCFG in our synthesized 10k COCO benchmark. Here, it is clear that CCFG generates higher quality images aligned with the positive prompt *while* being comparable at avoiding concepts in the negative

Method	FID	pos. prompt[↑]		neg. prompt[↓]	
		HPSv2	GPT4	HPSv2	GPT4
None	19.616	0.265	0.843	0.214	0.301
nCFG	21.064	0.259	0.788	0.199	0.148
CCFG	19.963	0.265	0.829	0.204	0.153

Table 3. Qualitative evaluation results on synthesized positive and negative prompt pairs with 10k COCO captions.

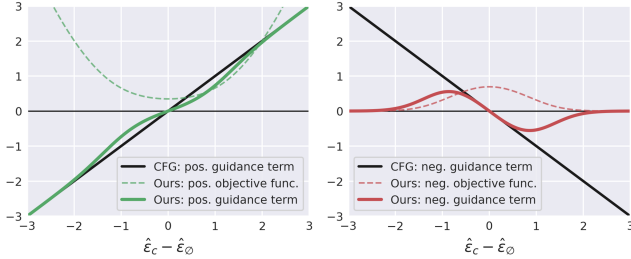


Figure 6. (a) The plot of the utilized objective function and a guidance term in traditional CFG and the proposed contrastive loss, in positive guidance (left) and negative guidance (right). (b) The dynamics of the effective guidance scale in the sampling process.

prompt.

5. Discussion

Analysis on guidance scale. We plot the guidance term and objective function of CCFG in Figure 6 as the difference between $\hat{\epsilon}_\emptyset$ and $\hat{\epsilon}_c$ changes. For visual simplicity, we considered the case of one-dimensional data. We also included the plot of the guidance term from CFG to visualize the difference between the behavior of the two sampling methods.

The contrastive loss for positive guidance is convex so that the denoising direction can be guided toward $\hat{\epsilon}_c$ via gradient descent. As $\|\hat{\epsilon}_c - \hat{\epsilon}_\emptyset\|$ increases, the guidance term approximates a linear function as the original CFG. On the other hand, the negative contrastive loss and its guidance term flatten out to 0 as $\|\hat{\epsilon}_c - \hat{\epsilon}_\emptyset\|$ gets bigger, while negated CFG diverges to infinity. This demonstrates the instability of the nCFG term, and how CCFG can resolve this issue by canceling the gradient guidance when $\hat{\epsilon}_\emptyset$ from the current sample x_t is sufficiently unrelated to the condition.

The behavior of nCFG on different scenarios. So far, we’ve shown the theoretical pitfall of the nCFG and demonstrated its negative effect on the sample distribution and its quality. Meanwhile, we observed that the criticality of nCFG’s drawback has been mitigated as the learned data distribution and the nature of the used condition get more complex: the nCFG term completely shifts the sample distribution out from the marginal support in the toy example of Figure 3, but often produced reasonable images for T2I generation tasks. Indeed, many off-the-shelf implementa-

tions for the T2I generation model have used this guidance to this day for concept negation [1, 13, 24, 29, 42].

We insist that this phenomenon occurs for the following reasons: First, as the possible conditions become more diverse and their relationship with the data distribution becomes more complex, it becomes harder for the model to accurately parameterize the entire unconditional and conditional distribution. It is well known that many other T2I models perform relatively poorly for pure unconditional generation, and extra distribution sharpening with CFG is almost essential for acceptable image quality. When this happens, even an unbounded guidance term can enhance the sample, until it overshoots and introduces artifacts. For more simplified scenarios like MNIST where the model can accurately learn the target data distribution, the downside of nCFG has expressed significantly. The second reason comes from $p(c^-|\mathbf{x})^{-\gamma}$, the factor that nCFG introduced to the sampling distribution. In a class-conditioned dataset where each class doesn’t overlap too much, $p(c^-|\mathbf{x})$ can be close to 1 if the given image is sampled from class c^- . This contrasts $p(c^-|\mathbf{x})^{-\gamma}$ with different \mathbf{x} significantly and assigns a high probability for the region with low $p(c^-|\mathbf{x})$, even for \mathbf{x} with low marginal probability. On the other hand, a single image can be described by numerous different texts, therefore the magnitude of $p(c|\mathbf{x})$ for an image-text pair is small no matter how c well-describes the given image.

Nonetheless, we believe that the fundamental flaws of nCFG have been already demonstrated with various experiments, and a risk of failure still remains for T2I models.

6. Conclusion

In this work, we proposed CCFG, a sampling method to guide diffusion samples to satisfy or repel the given condition, by optimizing the denoising direction with contrastive loss. Through the experiments on various datasets, we showed that CCFG resolves the downsides of the widely used negated CFG term, resulting in high-quality samples while faithfully avoiding unwanted attributes. Despite its effective computational overload and performance, one limitation could be the absence of analytic closed-form sampling distribution that corresponds to the proposed CCFG sampling. It would be a possible future work to propose a negative guidance that allows a probabilistic interpretation while persisting the suggested advantages of CCFG. We believe that CCFG has the potential to be easily integrated and benefit various downstream applications that utilize negative sampling.

References

- [1] Mohammadreza Armandpour, Ali Sadeghian, Huangjie Zheng, Amir Sadeghian, and Mingyuan Zhou. Re-imagine

- the negative prompt algorithm: Transform 2d diffusion into 3d, alleviate janus problem and beyond. *arXiv preprint arXiv:2304.04968*, 2023. 2, 3, 8
- [2] Yuanhao Ban, Ruochen Wang, Tianyi Zhou, Minhao Cheng, Boqing Gong, and Cho-Jui Hsieh. Understanding the impact of negative prompts: When and how do they take effect? *arXiv preprint arXiv:2406.02965*, 2024. 3
- [3] Nicolas Carlini, Jamie Hayes, Milad Nasr, Matthew Jagielski, Vikash Sehwal, Florian Tramèr, Borja Balle, Daphne Ippolito, and Eric Wallace. Extracting training data from diffusion models. In *32nd USENIX Security Symposium (USENIX Security 23)*, pages 5253–5270, 2023. 3
- [4] Ting Chen, Simon Kornblith, Mohammad Norouzi, and Geoffrey Hinton. A simple framework for contrastive learning of visual representations. In *International conference on machine learning*, pages 1597–1607. PMLR, 2020. 4
- [5] Ting Chen, Simon Kornblith, Mohammad Norouzi, and Geoffrey Hinton. A simple framework for contrastive learning of visual representations. In *International conference on machine learning*, pages 1597–1607. PMLR, 2020. 2, 5
- [6] Zhaorun Chen, Yichao Du, Zichen Wen, Yiyang Zhou, Chenhang Cui, Zhenzhen Weng, Haoqin Tu, Chaoqi Wang, Zhengwei Tong, Qinglan Huang, et al. Mj-bench: Is your multimodal reward model really a good judge for text-to-image generation? *arXiv preprint arXiv:2407.04842*, 2024. 7
- [7] Hyungjin Chung, Jeongsol Kim, Michael Thompson McCann, Marc Louis Klasky, and Jong Chul Ye. Diffusion posterior sampling for general noisy inverse problems. In *International Conference on Learning Representations*, 2023. 2, 3
- [8] Hyungjin Chung, Suhyeon Lee, and Jong Chul Ye. Decomposed diffusion sampler for accelerating large-scale inverse problems. *arXiv preprint arXiv:2303.05754*, 2023. 2, 3, 1
- [9] Hyungjin Chung, Jeongsol Kim, Geon Yeong Park, Hyelin Nam, and Jong Chul Ye. Cfg++: Manifold-constrained classifier free guidance for diffusion models. *arXiv preprint arXiv:2406.08070*, 2024. 2, 3, 4
- [10] Prafulla Dhariwal and Alexander Quinn Nichol. Diffusion models beat GANs on image synthesis. In *Advances in Neural Information Processing Systems*, 2021. 1
- [11] Yilun Du, Conor Durkan, Robin Strudel, Joshua B Tenenbaum, Sander Dieleman, Rob Fergus, Jascha Sohl-Dickstein, Arnaud Doucet, and Will Sussman Grathwohl. Reduce, reuse, recycle: Compositional generation with energy-based diffusion models and mcmc. In *International conference on machine learning*, pages 8489–8510. PMLR, 2023. 2
- [12] Bradley Efron. Tweedie’s formula and selection bias. *Journal of the American Statistical Association*, 106(496):1602–1614, 2011. 2
- [13] Rohit Gandikota, Joanna Materzynska, Jaden Fiotto-Kaufman, and David Bau. Erasing concepts from diffusion models. In *Proceedings of the IEEE/CVF International Conference on Computer Vision*, pages 2426–2436, 2023. 2, 3, 8
- [14] Rohit Gandikota, Hadas Orgad, Yonatan Belinkov, Joanna Materzyńska, and David Bau. Unified concept editing in diffusion models. In *Proceedings of the IEEE/CVF Winter Conference on Applications of Computer Vision*, pages 5111–5120, 2024. 3
- [15] Michael Gutmann and Aapo Hyvärinen. Noise-contrastive estimation: A new estimation principle for unnormalized statistical models. In *Proceedings of the thirteenth international conference on artificial intelligence and statistics*, pages 297–304. JMLR Workshop and Conference Proceedings, 2010. 2, 4
- [16] Raia Hadsell, Sumit Chopra, and Yann LeCun. Dimensionality reduction by learning an invariant mapping. In *2006 IEEE computer society conference on computer vision and pattern recognition (CVPR’06)*, pages 1735–1742. IEEE, 2006. 4
- [17] Martin Heusel, Hubert Ramsauer, Thomas Unterthiner, Bernhard Nessler, and Sepp Hochreiter. Gans trained by a two time-scale update rule converge to a local nash equilibrium. *Advances in neural information processing systems*, 30, 2017. 6
- [18] Jonathan Ho and Tim Salimans. Classifier-free diffusion guidance. *arXiv preprint arXiv:2207.12598*, 2022. 1, 2, 3
- [19] Jonathan Ho, Ajay Jain, and Pieter Abbeel. Denoising diffusion probabilistic models. *Advances in Neural Information Processing Systems*, 33:6840–6851, 2020. 2, 5, 6
- [20] Aapo Hyvärinen and Peter Dayan. Estimation of non-normalized statistical models by score matching. *Journal of Machine Learning Research*, 6(4), 2005. 2
- [21] Zahra Kadkhodaie and Eero Simoncelli. Stochastic solutions for linear inverse problems using the prior implicit in a denoiser. *Advances in Neural Information Processing Systems*, 34:13242–13254, 2021. 2
- [22] Jeongsol Kim, Geon Yeong Park, Hyungjin Chung, and Jong Chul Ye. Regularization by texts for latent diffusion inverse solvers. *arXiv preprint arXiv:2311.15658*, 2023. 2
- [23] Jeongsol Kim, Geon Yeong Park, and Jong Chul Ye. Dream-sampler: Unifying diffusion sampling and score distillation for image manipulation. In *European Conference on Computer Vision*, pages 398–414. Springer, 2025. 2, 4
- [24] Felix Koulischer, Johannes Deleu, Gabriel Raya, Thomas Demeester, and Luca Ambrogioni. Dynamic negative guidance of diffusion models. *arXiv preprint arXiv:2410.14398*, 2024. 3, 4, 8, 2
- [25] Alex Krizhevsky, Geoffrey Hinton, et al. Learning multiple layers of features from tiny images. 2009. 6
- [26] Yann LeCun, Léon Bottou, Yoshua Bengio, and Patrick Haffner. Gradient-based learning applied to document recognition. *Proceedings of the IEEE*, 86(11):2278–2324, 1998. 6
- [27] Seongyun Lee, Seungone Kim, Sue Hyun Park, Geewook Kim, and Minjoon Seo. Prometheusvision: Vision-language model as a judge for fine-grained evaluation. *arXiv preprint arXiv:2401.06591*, 2024. 7
- [28] Tsung-Yi Lin, Michael Maire, Serge Belongie, James Hays, Pietro Perona, Deva Ramanan, Piotr Dollár, and C Lawrence Zitnick. Microsoft coco: Common objects in context. In *Computer Vision—ECCV 2014: 13th European Conference, Zurich, Switzerland, September 6–12, 2014, Proceedings, Part V 13*, pages 740–755. Springer, 2014. 7

- [29] Nan Liu, Shuang Li, Yilun Du, Antonio Torralba, and Joshua B Tenenbaum. Compositional visual generation with composable diffusion models. In *European Conference on Computer Vision*, pages 423–439. Springer, 2022. 3, 8
- [30] Ben Poole, Ajay Jain, Jonathan T. Barron, and Ben Mildenhall. Dreamfusion: Text-to-3d using 2d diffusion. *arXiv*, 2022. 3
- [31] Alec Radford, Jong Wook Kim, Chris Hallacy, Aditya Ramesh, Gabriel Goh, Sandhini Agarwal, Girish Sastry, Amanda Askell, Pamela Mishkin, Jack Clark, et al. Learning transferable visual models from natural language supervision. In *International conference on machine learning*, pages 8748–8763. PMLR, 2021. 7, 1
- [32] Javier Rando, Daniel Paleka, David Lindner, Lennart Heim, and Florian Tramèr. Red-teaming the stable diffusion safety filter. *arXiv preprint arXiv:2210.04610*, 2022. 3
- [33] Robin Rombach, Andreas Blattmann, Dominik Lorenz, Patrick Esser, and Björn Ommer. High-resolution image synthesis with latent diffusion models. In *Proceedings of the IEEE/CVF Conference on Computer Vision and Pattern Recognition*, pages 10684–10695, 2022. 4
- [34] Hadi Salman, Alaa Khaddaj, Guillaume Leclerc, Andrew Ilyas, and Aleksander Madry. Raising the cost of malicious ai-powered image editing. *arXiv preprint arXiv:2302.06588*, 2023. 3
- [35] Patrick Schramowski, Manuel Brack, Björn Deiseroth, and Kristian Kersting. Safe latent diffusion: Mitigating inappropriate degeneration in diffusion models. In *Proceedings of the IEEE/CVF Conference on Computer Vision and Pattern Recognition*, pages 22522–22531, 2023. 3
- [36] Vikash Sehwal, Caner Hazirbas, Albert Gordo, Firat Ozgenel, and Cristian Canton. Generating high fidelity data from low-density regions using diffusion models. In *Proceedings of the IEEE/CVF Conference on Computer Vision and Pattern Recognition*, pages 11492–11501, 2022. 3
- [37] Gowthami Somepalli, Vasu Singla, Micah Goldblum, Jonas Geiping, and Tom Goldstein. Diffusion art or digital forgery? investigating data replication in diffusion models. In *Proceedings of the IEEE/CVF Conference on Computer Vision and Pattern Recognition*, pages 6048–6058, 2023. 3
- [38] Jiaming Song, Chenlin Meng, and Stefano Ermon. Denoising diffusion implicit models. *arXiv preprint arXiv:2010.02502*, 2020. 2, 6
- [39] Jiaming Song, Arash Vahdat, Morteza Mardani, and Jan Kautz. Pseudoinverse-guided diffusion models for inverse problems. In *International Conference on Learning Representations*, 2023. 2
- [40] Yang Song, Jascha Sohl-Dickstein, Diederik P. Kingma, Abhishek Kumar, Stefano Ermon, and Ben Poole. Score-based generative modeling through stochastic differential equations. In *9th International Conference on Learning Representations, ICLR*, 2021. 2
- [41] Pascal Vincent. A connection between score matching and denoising autoencoders. *Neural computation*, 23(7):1661–1674, 2011. 2
- [42] Max Woolf. Stable diffusion 2.0 and the importance of negative prompts for good results, 2023. Accessed: 2023-10-31. 2, 3, 4, 8
- [43] Jing Wu, Trung Le, Munawar Hayat, and Mehrtash Harandi. Erasediff: Erasing data influence in diffusion models. *arXiv preprint arXiv:2401.05779*, 2024. 2, 3
- [44] Xiaoshi Wu, Yiming Hao, Keqiang Sun, Yixiong Chen, Feng Zhu, Rui Zhao, and Hongsheng Li. Human preference score v2: A solid benchmark for evaluating human preferences of text-to-image synthesis. *arXiv preprint arXiv:2306.09341*, 2023. 7, 1
- [45] Jiazheng Xu, Xiao Liu, Yuchen Wu, Yuxuan Tong, Qinkai Li, Ming Ding, Jie Tang, and Yuxiao Dong. Imagereward: Learning and evaluating human preferences for text-to-image generation. *Advances in Neural Information Processing Systems*, 36, 2024. 7, 1
- [46] Jiwen Yu, Yinhuai Wang, Chen Zhao, Bernard Ghanem, and Jian Zhang. Freedom: Training-free energy-guided conditional diffusion model. In *Proceedings of the IEEE/CVF International Conference on Computer Vision*, pages 23174–23184, 2023. 3
- [47] Gong Zhang, Kai Wang, Xingqian Xu, Zhangyang Wang, and Humphrey Shi. Forget-me-not: Learning to forget in text-to-image diffusion models. In *Proceedings of the IEEE/CVF Conference on Computer Vision and Pattern Recognition*, pages 1755–1764, 2024. 3
- [48] Yi Zhou, Yilai Li, Jing Yuan, and Quanquan Gu. Cryofm: A flow-based foundation model for cryo-em densities. *arXiv preprint arXiv:2410.08631*, 2024. 3

Contrastive CFG: Improving CFG in Diffusion Models by Contrasting Positive and Negative Concepts

Supplementary Material

A. Additional results

A.1. CCFG in perspective of guided sampling on the posterior mean.

Algorithm 2 DDIM sampling with CCFG on the posterior mean

Require: $\mathbf{x}_T \sim \mathcal{N}(0, \mathbf{I})$, $\{\rho_t\}_{t=1}^T > 0$, $\tau > 0$, mode $\in \{\text{'pos'}, \text{'neg'}\}$

- 1: Initialize $\mathbf{x}_t = \mathbf{x}_T$
- 2: **for** $i = T$ **to** 1 **do**
- 3: **if** mode == 'pos' **then**
- 4: $\lambda = \frac{2}{1 + e^{-\tau \|\hat{\epsilon}_{\mathcal{D}}(\mathbf{x}_t) - \hat{\epsilon}_{\mathcal{C}}(\mathbf{x}_t)\|^2}}$
- 5: **else**
- 6: $\lambda = -\frac{2e^{-\tau \|\hat{\epsilon}_{\mathcal{D}}(\mathbf{x}_t) - \hat{\epsilon}_{\mathcal{C}}(\mathbf{x}_t)\|^2}}{1 + e^{-\tau \|\hat{\epsilon}_{\mathcal{D}}(\mathbf{x}_t) - \hat{\epsilon}_{\mathcal{C}}(\mathbf{x}_t)\|^2}}$
- 7: **end if**
- 8: $\hat{\epsilon}_{\mathcal{C}}^{\rho_t}(\mathbf{x}_t) = \hat{\epsilon}_{\mathcal{D}}(\mathbf{x}_t) + \rho_t \lambda (\hat{\epsilon}_{\mathcal{C}}(\mathbf{x}_t) - \hat{\epsilon}_{\mathcal{D}}(\mathbf{x}_t))$
- 9: $\hat{\mathbf{x}}_{\mathcal{C}}^{\rho_t}(\mathbf{x}_t) = (\mathbf{x}_t - \sqrt{1 - \bar{\alpha}_t} \hat{\epsilon}_{\mathcal{C}}^{\rho_t}(\mathbf{x}_t)) / \sqrt{\bar{\alpha}_t}$
- 10: $\mathbf{x}_{t-1} = \sqrt{\bar{\alpha}_{t-1}} \hat{\mathbf{x}}_{\mathcal{C}}^{\rho_t}(\mathbf{x}_t) + \sqrt{1 - \bar{\alpha}_{t-1}} \hat{\epsilon}_{\mathcal{D}}(\mathbf{x}_t)$
- 11: **end for**
- 12: **return** \mathbf{x}_t

In the suggested algorithm of CCFG in Alg. 1, we applied the suggested contrastive loss to optimize the denoising direction $\hat{\epsilon}_{\mathcal{D}}(\mathbf{x}_t)$, with the same spirit of the conventional CFG that modifies $\hat{\epsilon}_{\mathcal{D}}(\mathbf{x}_t)$ directly. This enabled us to conduct a fair comparison with the conventional CFG using an equal guidance scale.

Meanwhile, recall that the motivation for constructing CCFG was to pose positive and negative prompt sampling as guided sampling similar to CFG++ [8], which optimizes the posterior mean $\hat{\mathbf{x}}_{\mathcal{D}}(\mathbf{x}_t)$ with the iteration of (6). In order to follow this scheme, one would have to use the null noise $\hat{\epsilon}_{\mathcal{D}}(\mathbf{x}_t)$ in the renoising process, as shown in lines 9~10 of Alg. 2.

Here, we show that these two different implementations can be equivalent with appropriate guidance scale scheduling. Considering a single DDIM reverse sampling step, the obtained \mathbf{x}_{t-1} from \mathbf{x}_t by Alg. 2 can be written as follows:

$$\mathbf{x}_{t-1} = \frac{1}{\sqrt{\alpha_t}} \mathbf{x}_t + \left(\sqrt{1 - \bar{\alpha}_{t-1}} - \frac{\sqrt{1 - \bar{\alpha}_t}}{\sqrt{\alpha_t}} \right) \hat{\epsilon}_{\mathcal{D}} - \rho_t \lambda \frac{\sqrt{1 - \bar{\alpha}_t}}{\sqrt{\alpha_t}} (\hat{\epsilon}_{\mathcal{C}} - \hat{\epsilon}_{\mathcal{D}}). \quad (24)$$

In contrast, in Alg. 1, the iteration reads

$$\mathbf{x}_{t-1} = \frac{1}{\sqrt{\alpha_t}} \mathbf{x}_t + \left(\sqrt{1 - \bar{\alpha}_{t-1}} - \frac{\sqrt{1 - \bar{\alpha}_t}}{\sqrt{\alpha_t}} \right) \hat{\epsilon}_{\mathcal{D}} - \omega \lambda \left(\sqrt{1 - \bar{\alpha}_{t-1}} - \frac{\sqrt{1 - \bar{\alpha}_t}}{\sqrt{\alpha_t}} \right) (\hat{\epsilon}_{\mathcal{C}} - \hat{\epsilon}_{\mathcal{D}}). \quad (25)$$

Therefore, by setting

$$\rho_t = \omega \left(1 - \frac{\sqrt{\alpha_t} \sqrt{1 - \bar{\alpha}_{t-1}}}{\sqrt{1 - \bar{\alpha}_t}} \right), \quad (26)$$

we can show the equivalence between Alg. 1 and Alg. 2. Hence, for a direct and fair comparison of CCFG against conventional CFG, we chose CCFG with Alg. 1 as our implementation.

A.2. Quantitative metrics for Text-to-Image negative sampling.

Tab. 4 shows the alignment between given text prompts and the images sampled with different negative sampling methods in four scenarios of positive and negative prompt pairs. For each scenario, 100 images were sampled with StableDiffusion 1.5. To quantify the alignment of the output image and the given prompt, we measured the CLIP cosine similarity score [31], ImageReward [45], HPS-v2 [44], and an image-text agreement score from a VLM of GPT4o-mini. The ideal behavior as an effective and safe negative sampling method is to maintain alignment with positive prompts while decreasing alignment with negative prompts, compared to when no negative guidance is applied.

In all four scenarios, DNG showed the smallest alignment metric decrease between its samples and the given positive prompt but failed to thoroughly rule out the features described in the negative prompt; the output images' alignment with the negative prompt was marginally decreased, and GPT4 often detected the contents of the negative prompt. Meanwhile, nCFG successfully removed unwanted features from the sampled images but also affected the alignment with the positive prompts. All alignment metrics with the positive prompt were decreased the most among the three sampling methods, and more than 10% of its output was judged to not satisfy the positive prompt by GPT4 in all scenarios. Our proposed CCFG removes the undesired properties enough to be undetected by GPT4, and still maintains the agreement with the positive prompts.

positive/negative prompt		Negative Guidance	pos. prompt[↑]				neg. prompt[↓]			
			CLIP	IR	HPS-v2	GPT4	CLIP	IR	HPS-v2	GPT4
“a photo of a flower.”	“a yellow flower.”	None	23.754	0.185	0.260	1.00	19.830	-1.825	0.213	0.10
		DNG	23.626	0.137	0.258	0.99	19.698	-1.838	0.211	0.09
		nCFG	18.662	-1.352	0.220	0.66	11.880	-2.268	0.158	0.00
		CCFG	22.696	-0.372	0.251	0.99	16.365	-2.249	0.184	0.00
“photo of a basket full of delicious fruits.”	“strawberries.”	None	26.776	0.964	0.322	0.99	16.383	-1.300	0.232	0.75
		DNG	26.323	0.880	0.312	1.00	15.574	-1.996	0.219	0.31
		nCFG	26.119	0.628	0.297	0.85	13.840	-2.218	0.192	0.01
		CCFG	26.194	0.812	0.314	1.00	14.508	-2.188	0.204	0.02
“an airplane flying through sky.”	“photo with clouds.”	None	22.130	0.207	0.258	0.99	17.203	-1.275	0.192	0.45
		DNG	22.069	0.197	0.257	0.99	16.930	-1.285	0.189	0.38
		nCFG	20.976	0.047	0.241	0.90	15.374	-2.014	0.173	0.01
		CCFG	21.192	0.206	0.246	0.96	15.551	-1.955	0.175	0.04
“a gorgeous English breakfast.”	“fried egg on a plate.”	None	24.083	-0.259	0.254	1.00	20.220	0.068	0.271	0.94
		DNG	24.036	-0.286	0.252	1.00	19.506	-0.117	0.266	0.87
		nCFG	20.226	-1.419	0.222	0.89	7.779	-2.248	0.179	0.00
		CCFG	22.181	-0.873	0.235	0.99	12.144	-2.114	0.205	0.03

Table 4. More qualitative evaluation results with 100 sampled images on each scenario in Figure 1.

A.3. Text-to-image negative sampling examples with CCFG.

In Figure 7, we display additional image generation scenarios with CCFG and given positive-negative prompt pairs. In this section, we include the samples from StableDiffusion 1.5 and StableDiffusion XL to demonstrate that our methodology of CCFG works well on more recent and large-scale models.

B. Experimental details

B.1. Sampling hyperparameters.

Tab. 5 lists the hyperparameter values used for DNG and CCFG for the results in the main manuscript. Apart from the guidance scale ω that is shared by all negative sampling methods we’ve tested, DNG requires a prior for the given condition $p(c)$, an affine transformation weight τ' and bias δ for its guidance term calculation. We first took the values from the authors of DNG [24] as a basis, then additionally searched and tuned for the best performance on each dataset. We note that DNG only showed acceptable performances with the heavily exaggerated condition prior $p(c)$ which are far from the reasonable value (e.g. 0.1 for MNIST and CIFAR10). In the case of CCFG’s temperature value, we used $\tau=0.2$ for all experiments.

B.2. GPT prompts for negative sampling benchmark generation and evaluation.

The following prompt 1 was used to evaluate the agreement between the given image and text prompt with GPT4o-mini. The last line of the output is interpreted as a fraction between 0 and 1, where 1 is the highest agreement score possible.

To synthesize a benchmark dataset of positive-negative

MNIST	
DNG	$p(c)=0.25, \tau'=0.25, \delta=0$
CCFG	$\tau=0.2$
CIFAR10	
DNG	$p(c)=0.25, \tau'=0.2, \delta=0.0002$
CCFG	$\tau=0.2$
StableDiffusion 1.5	
DNG	$p(c)=0.01, \tau'=0.2, \delta=0.003$
CCFG	$\tau=0.2$

Table 5. Sampling hyperparameters used for DNG and CCFG.

prompt pairs to evaluate negative sampling methods, we fed 10,000 text descriptions from COCO validation and test split with the following prompt 2. The VLM is required to decompose the contents in the given text, and then randomly select one of them to remove it from the original text. As a result, the VLM produces a synthesized positive prompt and an unwanted object as a negative prompt.

StableDiffusion 1.5



StableDiffusion XL



Figure 7. Examples of text-to-image generation results with positive-negative prompt pairs and CCFG, using StableDiffusion 1.5 and StableDiffusion XL.

prompt 1

I'll give you an image and a text prompt. You have to evaluate how well the image satisfies the prompt. In the process, you first list all the objects described in the prompt. Then, you observe the image and decide whether each detected object is contained in the image as described in the prompt. The last line of your response should be a format of "Final answer: A over B", where A is the number of objects that are contained in the image and B is the total number of objects in the prompt.

For example, if the prompt is "a blue cat and a red dog" and the image contains a blue cat and a yellow dog, the answer should be "1 over 2".

Now, the input sentence is "<caption>". Observed the given image and answer.

prompt 2

I'll give you a sentence that describes a scene containing multiple attributes like objects, colors, etc. Your job is to write a sentence such that one content is removed from the original sentence.

You first list all the objects described in the sentence with numbering, then pick one of the objects described in the sentence.

Then, return me two sentences. The first output should be a picked object. The second output should be a grammatically correct and complete sentence in which the picked object is removed, but similar to the original sentence for the remaining objects. When the second sentence is written, you should also erase the attributes belonging to the removed object. Precisely follow the format of the examples below.

Input: Painting of oranges, a bowl, a white candle, and a pitcher

Objects: oranges, a bowl, a white candle, a pitcher

Output1: a white candle

Output2: Painting of oranges, a bowl, and a pitcher

Input: A couple of street signs hanging on a pole

Objects: street signs, pole

Output1: pole

Output2: A couple of street signs.

Now, the input sentence is "<caption>".